Metrol. Meas. Syst., Vol. XXII (2015), No. 2, pp. 315–326.

METROLOGY AND MEASUREMENT SYSTEMS
Index 330930, ISSN 0860-8229
www.metrology.pg.gda.pl

ROUGHNESS PARAMETERS CALCULATION BY MEANS OF ON-LINE VIBRATION MONITORING EMERGING FROM AWJ INTERACTION WITH MATERIAL

Pavol Hreha[1], Agata Radvanska[1], Lucia Knapcikova[1], Grzegorz M. Królczyk[2], Stanisław Legutko[3], Jolanta B. Królczyk[2], Sergej Hloch[1, 4], Peter Monka[1]

1) Faculty of Manufacturing Technologies TUKE with a seat in Prešov, Bayerova 1, 080 01 Prešov (pavol.hreha2@gmail.com, radvanska.agata@gmail.com, knapcikova.lucia@gmail.com, peter.monka@tuke.sk)
2) Opole University of Technology, Faculty of Production Engineering and Logistics, Prószkowska 76, 45-758 Opole, Poland (✉ g.krolczyk@po.opole.pl, +48 77 449 8688, *j.krolczyk@po.opole.pl)*
3) Poznań University of Technology, Faculty of Mechanical Engineering and Management, Piotrowo 3, 60-965 Poznań, Poland (stanislaw.legutko@put.poznan.pl)
4) Institute of Geonics AS CR, v. v. i., Studentska 1768, Ostrava-Poruba, 708 00 (hloch.sergej@gmail.com)

Abstract

The paper deals with a study of relations between the measured *Ra*, *Rq*, *Rz* surface roughness parameters, the traverse speed of cutting head *v* and the vibration parameters, *PtP*, *RMS*, *vRa* , generated during abrasive water jet cutting of the AISI 309 stainless steel. Equations for prediction of the surface roughness parameters were derived according to the vibration parameter and the traverse speed of cutting head. Accuracy of the equations is described according to the Euclidean distances. The results are suitable for an on-line control model simulating abrasive water jet cutting and machining using an accompanying physical phenomenon for the process control which eliminates intervention of the operator.

Keywords: abrasive water jet, surface topography, material vibration, vibration measurement.

© 2015 Polish Academy of Sciences. All rights reserved

1. Introduction

At present, the progress of development of new structural materials moves at a rapid pace. Development of new materials requires constant attention of technologists regarding possibilities of their machining [1]. The technologists are forced to permanently focus on development and innovation of unconventional technologies capable of machining these new materials [2–5]. None of the well-known structural materials presents a more significant issue for *Abrasive Water Jet* cutting – AWJ. In spite of continuous attention of the researchers dealing with the technology, no functional model exists for on-line monitoring of the instant state of AWJ cutting process [6]. To create such a model, it is inevitable to understand processes occurring during the cutting. The process must be monitored [7] through indirect quantities. In the course of material cutting, producing outputs not for direct use can be observed. These secondary products include vibrations, [6–10] acoustic emission [7, 9, 11], thermal emission [12], *etc*. All of these quantities are carriers of information about the technological process. They carry encoded information on cutting conditions and characteristics of the cut material surface [13].

2. State of the Art

Cutting with AWJ [14–17] and with a pulsating jet [2, 4–6] which is recognized as unconventional means of material cutting was commercially developed in the 80s. The AWJ

Article history: received on Oct. 01, 2014; accepted on Apr. 20, 2015; available online on May 29, 2015; DOI: 10.1515/mms-2015-0024.
Unauthenticated
Download Date | 4/30/18 11:41 AM

issue is significant and is still a subject of concentrated research. In the final years of the previous century, the basic research was oriented towards description of removal mechanisms [16–18]. The AWJ technology is used in technological processes of drilling, lathe-turning and threading, as well as in the process of improving and development of new, widely-used applications, *e.g*. cryogenic cutting, 3D cutting, drilling, cutting without abrasive, and pulsating jet cutting. A great deal of research has been devoted to achieve better comprehension of physics of removal [16, 19]. The majority of developed models describe interaction between the AWJ and material [20]. This area of research is concentrated chiefly on understanding the removal mechanism, as well as an influence of the technological factors upon the surface topography, with the aim of their optimization; the pressure, traverse speed, abrasive mass flow rate, and flow being the most frequently evaluated causes [20, 22]. Fig. 1 shows the influence of individual technological factors upon one of the surface parameters. It refers to a significant influence of the traverse speed of cutting head with a rapid increase of its cutting depth. Fig. 1 illustrates the values of effects of the individual factors upon the final parameters for nineteen investigated depth lines.

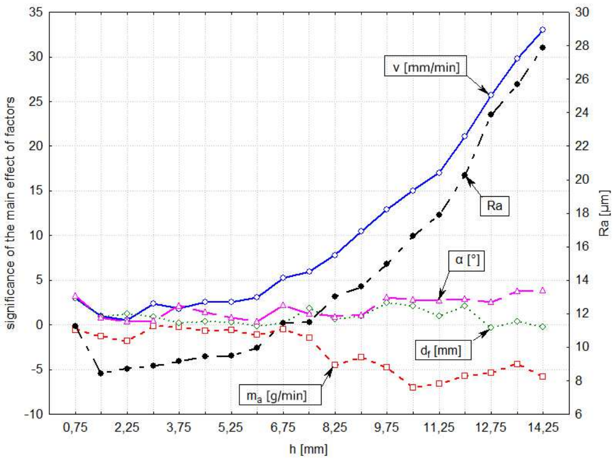

Fig. 1. The effect of factors on the surface profile parameter *Ra* [μm] (average value) in dependence on the depth of cut *h* [mm].

The graph (Fig. 1) is a result of the full factorial analysis with the range of factor setting as follows: v = 50–150 mm/min, m_a = 250–400 g/min, d_f = 0.8–1.4 mm and α = 0°–90. Along with the increased depth, an effect of the factor upon the traverse speed of cutting head also grows significantly (blue curve). A negative effect was observed for the factor of abrasive mass flow rate m_a. Increasing this factor results in decreasing the value of the investigated surface parameter. A sharp increase of the effect of individual factors with increasing the depth *h* [mm] is caused by losing the tool's kinetic energy and by consequent deformation in the cutting process (Fig. 1).

During AWJ cutting, mechanical vibrations are generated by local deformation in the stressed material. Due to the fact that the material is under erosive influence of AWJ, using the vibration analysis in the case of its application and monitoring material cutting by AWJ appears to be ideal. In the past, some authors published studies presenting applications of vibrations, or acoustic emission, for the purpose of on-line control and monitoring of an instant state of formed cut and its morphology [9, 23]. More authors dealt with the issue in the past. In 1992 Kovacevic [23] concentrated on indirect depth monitoring of penetration into a wooden material. Normal forces acting on a workpiece and generated by AWJ were used as

Unauthenticated
Download Date | 4/30/18 11:41 AM

indirect indicators. Wilcox *et al*. [7] dealt with the issue of cutting tool wear in the case of frontal milling. During monitoring, a combination of acoustic emission and cutting force was applied. Momber *et al*. [24] employed acoustic emission for on-line monitoring of the AWJ cutting of materials damaged by fracture. For the quantitative measurement of dispersed energy, the *RMS* value was used. Ravishankar [25] employed the *RMS* value of acoustic emission in the case of drilling composite laminates. Tönshoff *et al*. [11] used acoustic emission for monitoring processes of lathe-turning and grinding. Later, Asraf *et al*. [26] designed a model for on-line monitoring of the depth of cutting in the AWJ process through acoustic emission. The same model observed that the RMS value increased linearly with increasing the depth of cutting. Monno *et al*. [8] applied the analysis of vibrations in the case of AWJ cutting with using an oscillation technique in order to remove kerfs on the cutting edge. The relation between generated high-pressure jet and acoustic waving was studied by Foldyna *et al*. [2].

3. Experimental setup

Technological conditions of the experiment are shown in Table 1. The following factors were taken for evaluation: traverse speed v, abrasive mass flow rate m_a, and focusing tube diameter d_f. During cutting of experimental samples the cut material vibrations were monitored. The sensors were fixed, as shown in Fig. 2. Collecting data was performed by an NI PXI–1031 system; NI PXI–6109 was used for simultaneous collecting data from eight channels with the sampling frequency of 30 kHz. A total of 16 square-shape samples were produced. The sets A and B of samples were produced by an unworn focusing tube, whereas the C and D sets were produced by a worn focusing tube. In the case of A and C sets the abrasive mass flow rate of m_a = 400 g/min was used, and in the case of B and D sets it was equal to m_a = 250 g/min.

The monitored signals were analysed by a virtual tool created in the object programming environment of LabVIEW.

Table 1. The technological conditions of experiments.

<table>
<tr><th colspan="3">Factors</th><th>Technological conditions</th></tr>
<tr><td colspan="3">Type of intensifier [FLOW 9xD55]</td><td>Double acting (PTV-37-60 PUMP)</td></tr>
<tr><td colspan="3">Power of intensifier [HP]</td><td>60</td></tr>
<tr><td colspan="3">Pressure in hydraulic circuit [MPa]</td><td>20</td></tr>
<tr><td colspan="3">Intensification ratio</td><td>20:1</td></tr>
<tr><td colspan="3">Maximal pressure [MPa]</td><td>415 MPa</td></tr>
<tr><td colspan="3">Water mass flow</td><td>3.68 l/min</td></tr>
<tr><td colspan="3">Cutting head type</td><td>Diamond cutting head PTV™</td></tr>
<tr><td colspan="3">Pressure p [MPa]</td><td>350</td></tr>
<tr><td colspan="3">Traverse speed v [mm/min]</td><td>150</td></tr>
<tr><td colspan="3">Abrasive mass flow rate m_a [g/min]</td><td>250, 400</td></tr>
<tr><td colspan="3">Water orifice diameter d_o [mm]</td><td>0.4</td></tr>
<tr><td colspan="3">Focusing tube diameter d_f [mm]</td><td>1.2</td></tr>
<tr><td colspan="3">Standoff distance z [mm]</td><td>3</td></tr>
<tr><td colspan="3">Angle of attack φ [°]</td><td>90</td></tr>
<tr><td colspan="3">Type of abrasive/MESH</td><td>Barton Garnet/80</td></tr>
<tr><td rowspan="2">Material</td><td rowspan="2">AISI 309
b = 15 mm</td><td>Chemical composition</td><td>(C 0.20%, Mn 2%, Si 1%, Cr 22 – 24%, Ni 12 – 15%, P 0,045%, S 0.03%)</td></tr>
<tr><td>Mechanical properties at room temperature</td><td>(Hardness – Brinell) 95, μ = 0.27–0.3, E = 200 GPa, σ_t = 515 MPa, σ_K = 205 MPa, Ductility A = 40%, Contraction Z = 50%)</td></tr>
</table>

Unauthenticated
Download Date | 4/30/18 11:41 AM

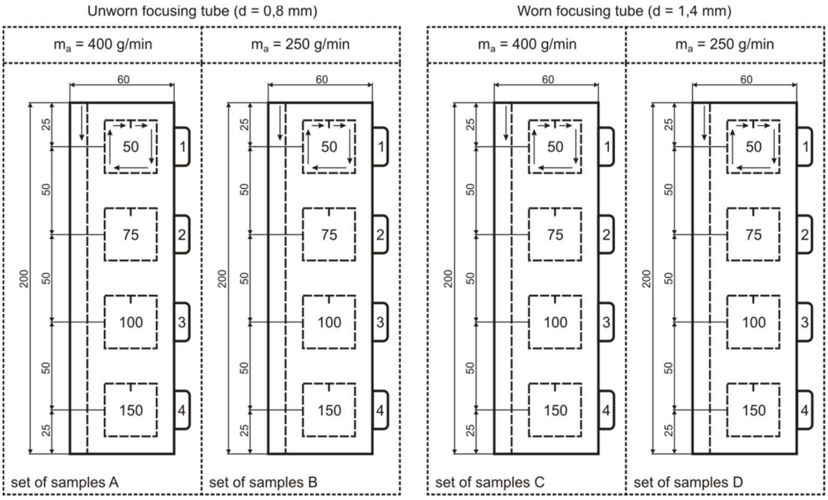

Fig. 2. The experimental design.

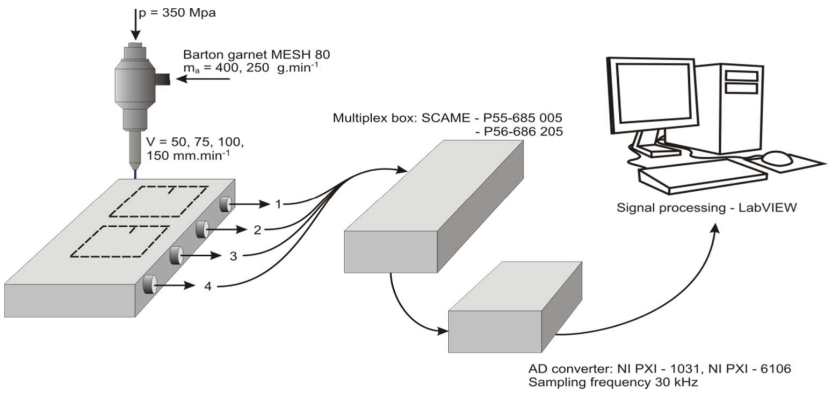

Fig. 3. The experimental methodology and on-line measurement during abrasive water jet cutting of samples (Fig. 2).

The topography of experimental samples was measured by a non-contact optical profilometer MicroProf FRT manufactured by Fries Research & Technology GmbH, Germany. The measured data were also processed by a virtual tool created in the object programming environment of LabVIEW. The topography parameters *Ra*, *Rq* and *Rz* were measured in three zones on a part of the sample. The arrangement of investigated zones is shown in Fig. 4.

The first and the last zones are 5 mm from the sample edges . The arrangement provided the measurement point before a shape change caused by changing the traverse direction of cutting head. The middle zone is 15 mm from the beginning of the investigated zone. The zone width corresponds − according to the standard − with the specified measuring length value of 2.5 mm. The parameters were measured in nineteen lines with equidistance of 0.75 mm. The first measured line is also in the distance of 0.75 mm from the upper edge of the sample.

Unauthenticated
Download Date | 4/30/18 11:41 AM

4. Results and discussion

To describe a relation between the technological factor, parameters of material vibrations and final parameters of surface topography, a polynomial multi-parametric regression was performed. In the case of deriving the equation it is assumed that the final surface roughness parameter is a function of the traverse speed *v* and the material vibrations. These individual functional dependences are represented by the functions (1) and (2).

$$f_{(x)} = a_0 + a_1 x^1 + a_2 x^2 + a_3 x^3 \cdots a_{n-1} x^{n-1} + a_n x^n, \tag{1}$$

$$f_{(y)} = a_0 + a_1 y^1 + a_2 y^2 + a_3 y^3 \cdots a_{n-1} y^{n-1} + a_n y^n. \tag{2}$$

As the function of one dependent and two independent variables has a form (3), it is necessary to make a substitution to calculate a combination of terms from x_1 up to x_{15}.

$$f_{(x;y)} = a_{00} + a_{10}x^1 + a_{20}x^2 + a_{30}x^3 + a_{01}y + a_{02}y + a_{03}y + a_{11}xy + a_{12}xy^2 + a_{13}xy^3 + a_{21}x^2y + \\ + a_{22}x^2y^2 + a_{23}x^2y^3 + a_{31}x^3y + a_{32}x^3y^2 + a_{33}x^3y^3. \tag{3}$$

Substitution:

$x_1 = x^1 \; m_1 = a_{10}$	$x_6 = y^3 \; m_6 = a_{03}$	$x_{11} = x^2y^2 \; m_{11} = a_{22}$	$m_0 = a_{00}$
$x_2 = x^2 \; m_2 = a_{20}$	$x_7 = xy \; m_7 = a_{11}$	$x_{12} = x^2y^3 \; m_{12} = a_{23}$	
$x_3 = x^3 \; m_3 = a_{30}$	$x_8 = xy^2 \; m_8 = a_{12}$	$x_{13} = x^3y \; m_{13} = a_{31}$	
$x_4 = y^1 \; m_4 = a_{01}$	$x_9 = xy^3 \; m_9 = a_{13}$	$x_{14} = x^3y^2 \; m_{14} = a_{32}$	
$x_5 = y^2 \; m_5 = a_{02}$	$x_{10} = x^2y \; m_{10} = a_{21}$	$x_{15} = x^3y^3 \; m_{15} = a_{33}$	

After inserting the terms into the substituted function (4) it is possible to calculate its coefficients through the linear polynomial regression.

$$f_{(x)} = m_0 + m_1x_1 + m_2x_2 + m_3x_3 + m_4x_4 + m_5x_5 + m_6x_6 + m_7x_7 + m_8x_8 + m_9x_9 + m_{10}x_{10} + m_{11}x_{11} + m_{12}x_{12} + \\ + m_{13}x_{13} + m_{14}x_{14} + m_{15}x_{15}. \tag{4}$$

When the substituents were replaced by the original terms, the final function was expressed by the (4). The traverse speed of cutting head v was determined as the technological factor. That factor proved to influence the values of vibration parameters the most. The graphs in Fig. 4 refer to a significant influence of the traverse speed of cutting head upon the surface texture of the generated surface.

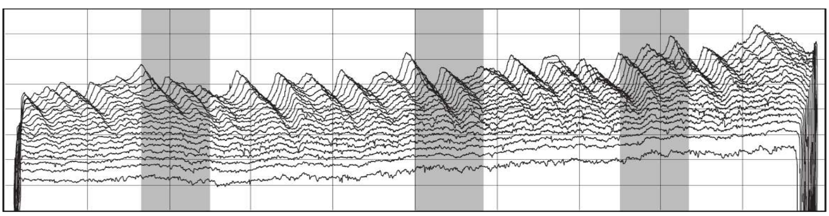

Fig. 4. The measured areas of sample surface texture on created with setting the AWJ factors: v = 150 mm/min, m_a = 400 g/min, d_f = 0.8 mm.

Unauthenticated
Download Date | 4/30/18 11:41 AM

Besides an impact upon the individual parameters, the traverse speed v of cutting head is an easily adjustable factor in the process of AWJ. The average values of the measurements in the depth line of 7.2 mm from the upper part of the sample were applied as the parameter values of surface topography in the case of regression. These values were assessed as dependent variables. The polynomial regression developed further to the third stage. As it is the case of a multi-parametric regression, the substitution of input parameters was performed, which allowed linearization. Consequently, the regression coefficients were calculated by means of the method of the smallest squares. These coefficients were inserted into the final regression equation. The regression coefficients of final equations are presented in Table 2. As the regression is non-linear, closeness of correspondence of the derived equations was assessed through Euclidean distances which show the deviation of the calculated values from the measured ones.

Table 2. The coefficients for correlation (5), (6) and (7).

	Coefficients for (5)	Coefficients for (6)	Coefficients for (7)
a_{00}	–1523.7773	–343.8886	770729.6532
a_{10}	–141.4949	–5.509	–18786.4002
a_{20}	2.6977	0.8554	150.7975
a_{30}	–0.0117	–0.005	–0.3985
a_{01}	19229.0397	33168.4348	–749957.2303
a_{02}	–51640.7423	–71166.9842	227210.0571
a_{03}	0	0	–20215.2502
a_{11}	2107.0835	198.1441	–16684.6492
a_{21}	–38.6258	–9.7115	–119.5139
a_{31}	0.161	0.0496	0.2783
a_{12}	–11521.8151	–2497.2044	–4242.8944
a_{22}	198.8332	52.993	22.5789
a_{32}	–0.8047	–0.2275	–0.0295
a_{13}	21326.1801	6128.7506	–229.7317
a_{23}	–348.3285	–97.0831	0.4665
a_{33}	1.3793	0.3787	–0.0073

4.1. Deriving equation for Ra parameter

The traverse speed of the cutting head and the average of absolute values of acceleration amplitudes were selected as independent factors for the polynomial multi-parametric regression of *Ra* parameter. The parameter of vibration signal was selected for similarity of its calculation with the mechanism of *Ra* calculation. The dependence of *Ra* parameter on variable quantities is described by the (5). The regression coefficients ranging from a_{00} to a_{33} are presented in Table 2.

Validity of the regression equation is limited by the range of input data. The final equation is a function of area (Fig. 5). According to descending area, in the case of increasing the average of absolute values of amplitudes, a positive influence of material vibrations upon the surface topography is possible to be deduced. The traverse speed of cutting head has an opposite effect, for the value of *Ra* parameter increases with an increase of the factor value.

$$Ra = a_{00} + a_{10}v + a_{20}v^2 + a_{30}v^3 + a_{01}v_{Ra} + a_{02}v_{Ra}^2 + a_{03}v_{Ra}^3 + a_{11}vv_{Ra} + a_{21}v^2v_{Ra} + \\ + a_{31}v^3v_{Ra} + a_{12}vv_{Ra}^2 + a_{22}v^2v_{Ra}^2 + a_{32}v^3v_{Ra}^2 + a_{13}vv_{Ra}^3 + a_{23}v^2v_{Ra}^3 + a_{33}v^3v_{Ra}^3. \tag{5}$$

Unauthenticated
Download Date | 4/30/18 11:41 AM

Accuracy of the regression equation is described by the graph shown in Fig. 6. It presents the difference between the predicted values and the values obtained by the measurement of surface roughness parameters. The variety of values referring to inaccuracy is obvious. As per the Euclidean distances, the deviation of the calculated and measured values is of 2.9 µm.

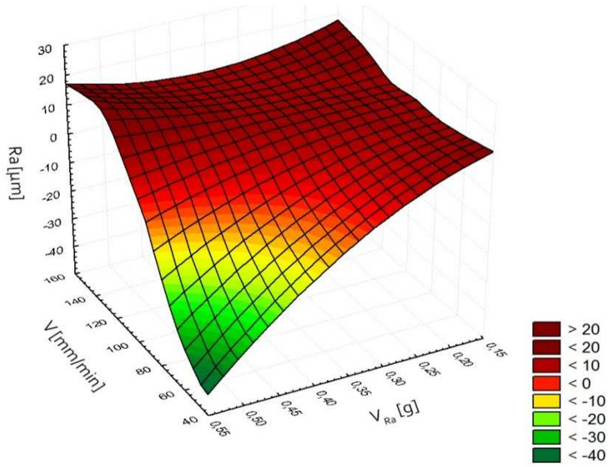

Fig. 5. Dependence of the surface roughness parameter *Ra* on the average of absolute values of material vibrations v_{Ra} and the traverse speed of cutting head v appertaining to the relation (5).

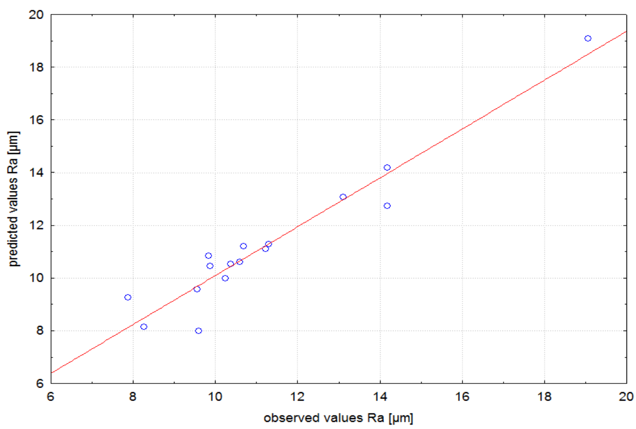

Fig. 6. The predicted and observed values of surface roughness parameters *Ra* according to (5).

4.2. Deriving equation for Rq parameter

Dependence on prediction of the middle quadratic deviation of the *Rq* profile was generated by regression of two variables. Similarly to the previous case, the technological factor was the traverse speed of cutting head. The so-called effective value of *RMS* vibrations was used as the material vibration parameter. The procedure of the value calculation is identical with that of the *Rq* value calculation. The coefficients ranging from a_{00} to a_{33} are also presented in Table 2. The area determined by the function is shown in the graph (Fig. 7). Contrary to the area describing dependence on the *Ra* parameter, its development is less smooth. The increased values of *Rq* at a higher speed are more visible. A positive influence of the roughness factor is obvious as well. The calculated and measured values of the *Rq*

Unauthenticated
Download Date | 4/30/18 11:41 AM

parameter in the graph (Fig. 8) refer to accuracy of the regression equation, which is higher in comparison with (5). The deviation of the calculated values from the ones measured for (6) is, according to Euclidean distances, of 1.4 µm.

$$Rq = a_{00} + a_{10}v + a_{20}v^2 + a_{30}v^3 + a_{01}RMS + a_{02}RMS^2 + a_{03}RMS^3 + a_{11}vRMS + a_{21}v^2RMS + \\ + a_{31}v^3RMS + a_{12}vRMS^2 + a_{22}v^2RMS^2 + a_{32}v^3RMS^2 + a_{13}vRMS^3 + a_{23}v^2RMS^3 + \\ + a_{33}v^3RMS^3. \quad (6)$$

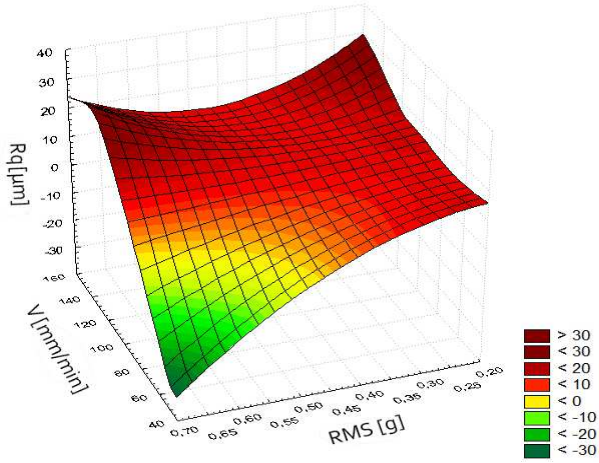

Fig. 7. Dependence of the surface roughness parameter *Rq* on the average of absolute values of material vibrations *RMS* and the traverse speed of cutting head *v* appertaining to (5).

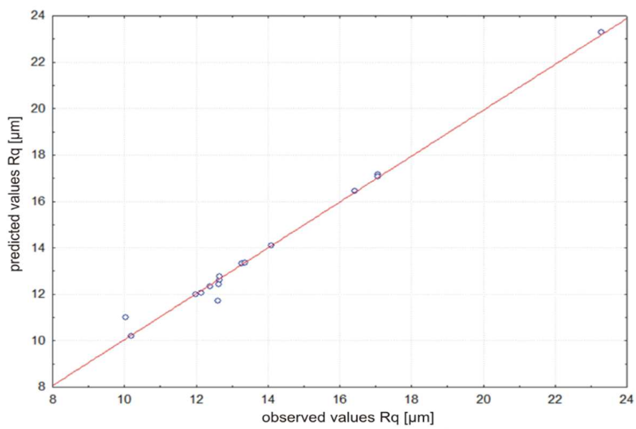

Fig. 8. The predicted and observed values of surface roughness parameters *Rq* according to (5).

4.3. Deriving equation for Rz parameter

The last studied equation is dependence of the height of profile roughness *Rz* on the variable factors. The traverse speed of the cutting head *v* and the parameter of vibration signal *Peak-to-Peak PtP* were used as independent variables. The final equation is given by the (7). The regression coefficients ranging from a_{00} to a_{33}, are, as well as in the previous cases, shown in Table 2.

Unauthenticated
Download Date | 4/30/18 11:41 AM

$$Rz = a_{00} + a_{10}v + a_{20}v^2 + a_{30}v^3 + a_{01}PtP + a_{02}PtP^2 + a_{03}PtP^3 + a_{11}vPtP + a_{21}v^2PtP + a_{31}v^3PtP$$
$$+ a_{12}vPtP^2 + a_{22}v^2PtP^2 + a_{32}v^3PtP^2 + a_{13}vPtP^3 + a_{23}v^2PtP^3 + a_{33}v^3PtP^3. \quad (7)$$

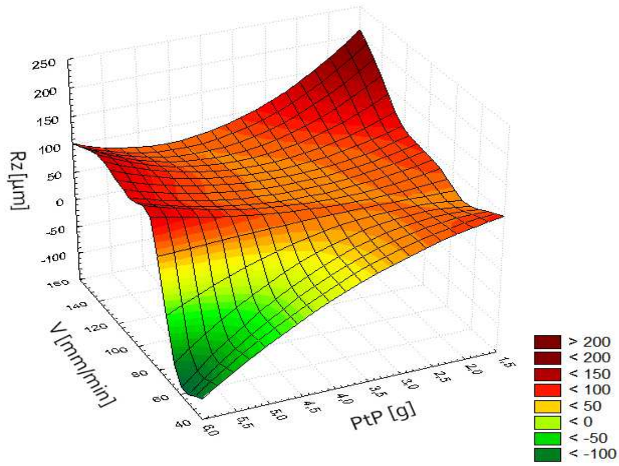

Fig. 9. Dependence of the surface roughness parameter *Rz* on the average of absolute values of material vibrations *Peak-to-Peak* and the traverse speed of cutting head *v* appertaining to (5).

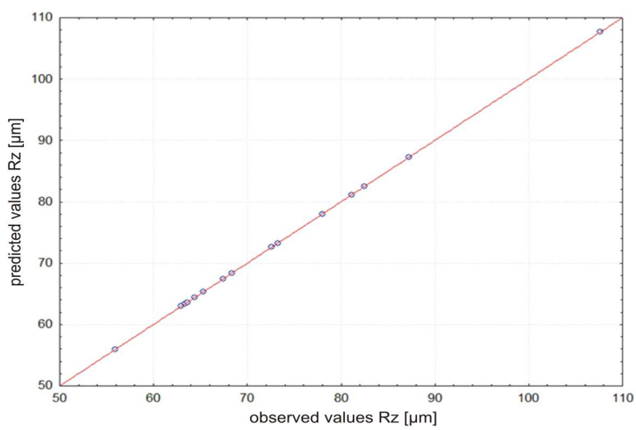

Fig. 10. The predicted and observed values of surface roughness parameters *Rz* according to (7).

The values calculated by the (7) are shown graphically in the area in Fig. 9. In the area, the waviness is demonstrated most distinctively. Similarly to the previous cases, a positive influence of vibrations upon the generated surface quality, and a negative effect of the traverse speed, are possible to be deduced. The highest values of surface roughness parameters can be observed at the maximum traverse speed from the range and at the lowest observed values of vibration parameters. Accuracy of (7) is graphically described in Fig. 10. In this case, the correlation is highly accurate. According to the Euclidean distances, the deviation of the calculated values from the measured ones is of 1.2E−8 µm.

5. Potential applications and future direction of research

Pursuant to the influences of the investigated technological factors, and by means of the prediction, (6) and (7), it is possible to predict the level of vibration parameters of cut

Unauthenticated
Download Date | 4/30/18 11:41 AM

material. These equations are applicable within the investigated range of factors for materials with E = 200 GPa and the thickness of up to 15 mm, as it is in the case of stainless steel AISI 309. Through regression between the traverse speed v [mm/min] of cutting head and the parameters of vibrations, *RMS*, *vRa,* the equations for prediction of the surface roughness parameter *Ra*, *Rq* and *Rz* values were detected.

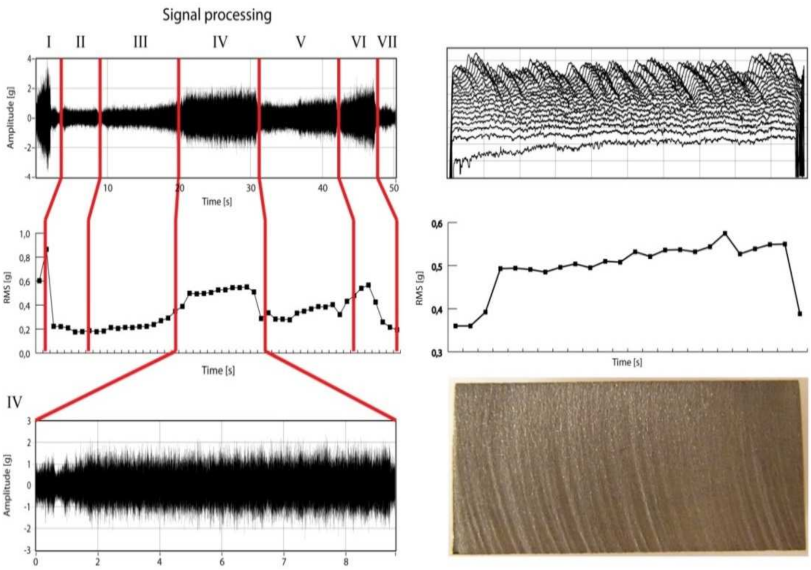

Fig. 11. The connection between the parameters of generated surface and the parameters of cut material vibrations.

By means of these polynomial dependences, the final value of the roughness parameter *Ra* of the generated surface is possible to be estimated with a defined defect. Following the description of previous studies and recently published studies by the authors dealing with the issue of AWJ cutting, it is clear that their attention is paid chiefly to prediction of the cutting depth without an option of the surface quality control. The presented equations for surface roughness parameters did not include the quantities describing the process in real time. Thus, they are unsuitable for a proposal of an on-line control that takes into consideration the quality of generated surface. At the same time, an influence of technological factors of AWJ upon parameters of secondary emission (vibrations) was not thoroughly studied. For consequent prediction of calculations and for the needs of an on-line control of AWJ technology, it is necessary to verify the implicitly recorded hypothesis and factors expressed in the implicit (8). The connection between the parameters of generated surface and the parameters of material vibrations is shown in Fig. 11.

$$Ra, Rq, Rz = f\left(v_{Ra}, RMS, PtP, v, d_f, m_a, E, p, b, \alpha\right). \tag{8}$$

Through prediction of surface quality by means of vibrations, it is possible to solve practical problems which most of engineers face in the technological process of AWJ cutting; solving them would be beneficial for maximization of the production performance and for setting the values of process parameters that would bring the required product quality. Using vibrations to determine the cutting performance will significantly help an operator in the decision making department. The technology control is based mainly upon the experience of the operator which represents a rather important cost for a company. Due to the

Unauthenticated
Download Date | 4/30/18 11:41 AM

aforementioned, it is inevitable to utilize secondary emission in the on-line process as a new method and strategy with the aim of predicting the cutting process and of regulating the surface roughness in real time.

6. Conclusion

The AWJ technology is currently the sole alternative for cutting some specific materials. In spite of its advantages, it has some drawbacks as well, as any other technology. Development of a new equipment and innovations to eliminate these drawbacks has invariably been an object of interest of researchers all around the world. This study contributes to clarification of queries related to connections between input technological factors, final parameters of surface roughness *Ra, Rq, Rz* and a secondary product of the process, the material vibrations. The biggest influence on the cut surface topography along the entire cross-section was observed in the case of the factor of the traverse speed of cutting head. Therefore, it was applied in the polynomial multi-parametric regression of two independent and one dependent variables. Surface roughness parameters were selected as independent variables which were assessed as a function of technological factor and as vibration parameters. The parameter of mean of absolute values of amplitudes was used for the *Ra* parameter. In the case of the *Rq* parameter, the *RMS* parameter was applied, whereas for the *Rz* parameter the Peak to Peak parameter was selected. Deviation of the calculated values from the measured ones according to final equations was assessed by the Euclidean distances. The deviation values were rather low and in the case of calculation of *Rz* parameter, the deviation was negligible. To solve this issue, it is inevitable to extend the scope of validity of regression equations in the future; it can be achieved through additional experiments, including several suggestible technological factors with a suitable range of set values. At the same time it is required to employ more types of materials with diverse mechanical properties into the experiments. Further on, it is appropriate to map out a complete technology by the analysis of vibration, and to assign to the individual equipment their appertaining frequencies and, subsequently, to identify transfer of these vibrations to the cut material. Successively, it will be necessary to synthetize the knowledge into a proposal of the feedback control, according to the continuous measurement of vibration parameters. The control circuit will provide regulation of the traverse speed of cutting head, as well as regulation of the roughness parameters that will be in the functional equation towards vibrations $Frq = f(Ra)$.

Acknowledgements

This work was supported by the Slovak Research and Development Agency under the contract No. APVV-207-12 and VEGA 1/0972/11. The measurements have been carried out with a support of the Institute of clean technologies for mining and utilization of raw materials for energy use, Reg. No. CZ.1.05/2.1.00/03.0082 supported by the Research and Development for Innovations Operational Programme financed by the Structural Funds of the European Union and the State budget of the Czech Republic, and with a support for the long term conceptual development of the research institution RVO: 68145535.

References

[1] Królczyk, G.M., Niesłony, P., Legutko, S. (2015). Determination of tool life and research wear during duplex stainless steel turning. *Archives of Civil and Mechanical Engineering*, 15(2), 347–354.

[2] Foldyna, J. Sitek, L., Scucka, J., Martinec, P., Valicek, J., Palenikova, K. (2009). Effects of pulsating water jet impact on aluminium surface. *Journal of Materials Processing Technology*, 209, 6174–6180.

Unauthenticated
Download Date | 4/30/18 11:41 AM

[3] Sharma, V., Chattopadhyaya, S., Hloch, S. (2011). Multi response optimization of process parameters based on Taguchi-Fuzzy model for coal cutting by water jet technology. *The Inter. J. of Adv. Manufact. Tech.*, 56(9–12), 1019–1025.

[4] Foldyna, J., Klich, J., Hlavacek, P., Zelenak, M., Scucka, J. (2012). Erosion of metals by pulsating water jet. *Tehnički vjesnik*, 19, 381–386.

[5] Riha, Z., Foldyna, J. (2012). Ultrasonic pulsation of pressure in a water jet cutting tool. *Tehnički vjesnik*, 19, 487–491.

[6] Hreha, P., Radvanská A., Hloch S., Peržel V., Królczyk G., Monková K. (2015). Determination of vibration frequency depending on abrasive mass flow rate during abrasive water jet cutting. *The Inter. J. of Advan. Manufact. Tech.,* 77, 763–774.

[7] Wilcox, S.J., Reuben, R.L., Souquet, P. (1997). The use of cutting force and acoustic emission signals for the monitoring of tool insert geometry during rough face milling. *Inter. J. of Mach. Tools and Manufact.*, 37(4), 481–494.

[8] Monno, M., Ravasio, C. (2005). The effect of cutting head vibrations on the surfaces generated by waterjet cutting. *Intern. J. of Mach. Tools and Manufact.*, 45(3), 355–363.

[9] Perzel, V., Hreha, V., Hloch, S, Tozan, H., Valicek, J. (2011). Vibration emission as a potential source of information for abrasive waterjet quality process control. *The Intern. J. of Advan. Manufact. Tech.*, 61(1–4), 285–294.

[10] He, W., Xu, G., Rong, Z., Li, G., Liu, M. (2014). Automatic calibration system for digital – display vibrometers based on machine vision. *Metrol. Meas. Syst.*, 21(2), 317–328.

[11] Tonshoff, H.K., Jung, M., Männel, S., Reitz, W. (2000). Using acoustic emission signals for monitoring of production processes. *Ultrasonics*, 37, 681–686.

[12] Babu, M., K., Chetty, O.V.K., (2002). Studies on recharging of abrasives in abrasive water jet machining. *The Inter. J. of Advan. Manufact. Tech.*, 19, 697–703.

[13] Brezina, I. (1991). Surface roughness, importance of roughness quantify – metrology aspects – development trends. *Jo.of Fine Mech. Opt.*, 7, 245–255.

[14] Arola, D. Ramulu, M. (1997). Material removal in abrasive waterjet machining of metals surface integrity and texture. *Wear*, 210, 50–58.

[15] Azmir, M.A., Ahsan, A.K. (2008). Investigation on glass/epoxy composite surfaces machined by abrasive water jet machining. *J. of Mater. Proc. Tech.*, 198, 122–128.

[16] Bitter, J. (1963). A study of erosion phenomena. Part I. *Wear*, 6, 5–21.

[17] Boud, F., Carpenter, C, Folkes, J, Shipway, P.H. (2010). Abrasive waterjet cutting of a titanium alloy: The influence of abrasive morphology and mechanical properties on workpiece grit embedment and cut quality. *J. of Mater. Proce. Tech.*, 210, 2197–2205.

[18] Kong, M.C., Axinte, D., Voice, W. (2010). Aspects of material removal mechanism in plain waterjet milling on gamma titanium aluminide. *J. of Mater. Proc. Tech.*, 210, 573–584.

[19] Fowler, G., Pashby, I.R., Shipway, P.H., (2009). The effect of particle hardness and shape when abrasive water jet milling titanium alloy Ti6Al4V. *Wear*, 266, 613–620.

[20] Hashish, M. (1991). Optimization factors in abrasive waterjet machining. *Journal of Engineering for Industry-Transactions of the ASME*, 113, 9–37.

[21] Vikram, G., Babu, N.R. (2002). Modelling and analysis of abrasive water jet cut surface topography. *Intern. J. of Machine Tools and Manufact.*, 42, 1345–1354.

[22] Chiffre De L., Lonardo, P., Trumpold, H., Lucca, D.A., Goch, G., Brown, C.A., Raja, J. Hansen, H.N. (2000). Quantitative characterisation of surface texture. *Annals of the CIRP*, 49(2), 635–642.

[23] Kovacevic, R. (1992). Monitoring the depth of abrasive waterjet penetration. *Inter. J. of Machine Tools and Manufacture*, 32(5), 725–736.

[24] Momber, A.W., Mohan, R.S., Kovacevic, R. (1999). On-line analysis of hydro-abrasive erosion of pre-cracked materials by acoustic emission. *Theoretical and Applied Fracture Mechanics*, 17(31), 1–17.

[25] Ravishankar, S.R., Murthy, C.R.L. (2000). Application of acoustic emission in drilling of composite laminates. *NDT&E International*, 33, 101–110.

[26] Asraf, I., Hassan, A.I., Chen, C., Kovacevic, R. (2004). On-line monitoring of depth of cut in AWJ cutting. *Intern. J. of Machine Tools and Manufact.*, 44, 595–605.

Unauthenticated
Download Date | 4/30/18 11:41 AM